A&A 529, A117 (2011)
DOI: 10.1051/0004-6361/201116673

Astronomy & Astrophysics

A *Herschel*⋆ resolved far-infrared dust ring around HD 207129

J. P. Marshall[1], T. Löhne[2], B. Montesinos[3], A. V. Krivov[2], C. Eiroa[1], O. Absil[4,⋆⋆], G. Bryden[5], J. Maldonado[1], A. Mora[6,1], J. Sanz-Forcada[3], D. Ardila[7], J.-Ch. Augereau[8], A. Bayo[9], C. del Burgo[10], W. Danchi[11], S. Ertel[12], D. Fedele[1,13,14], M. Fridlund[15], J. Lebreton[8], B. M. González-García[16], R. Liseau[17], G. Meeus[1], S. Müller[2], G. L. Pilbratt[15], A. Roberge[11], K. Stapelfeldt[5], P. Thébault[18], G. J. White[19,20], and S. Wolf[12]

[1] Departmento Física Teórica, Facultad de Ciencias, Universidad Autónoma de Madrid, Cantoblanco, 28049 Madrid, Spain
e-mail: jonathan.marshall@uam.es
[2] Friedrich-Schiller-Universität Jena, Astrophysikalisches Institut und Universitätssternwarte, 07743 Jena, Germany
[3] Departmento de Astrofísica, Centro de Astrobiología (CAB, CSIC-INTA), ESAC Campus, PO Box 78, 28691 Villanueva de la Cañada, Madrid, Spain
[4] Institut d'Astrophysique et de Géophysique, Université de Liège, 17 Allée du Six Août, 4000 Sart Tilman, Belgium
[5] Jet Propulsion Laboratory, California Institute of Technology, Pasadena, CA 91109, USA
[6] ESA-ESAC Gaia SOC. PO Box 78 28691 Villanueva de la Cañada, Madrid, Spain
[7] NASA Herschel Science Center, California Institute of Technology, 1200 E. California Blvd., Pasadena, CA 91125, USA
[8] UJF-Grenoble 1 / CNRS-INSU, Institut de Planétologie et d'Astrophysique de Grenoble (IPAG) UMR 5274, 38041 Grenoble, France
[9] European Space Observatory, Alonso de Cordova 3107, Vitacura, Casilla 19001, Santiago 19, Chile
[10] UNINOVA-CA3, Campus da Caparica, Quinta da Torre, Monte de Caparica, 2825-149 Caparica, Portugal
[11] NASA Goddard Space Flight Center, Exoplanets and Stellar Astrophysics, Code 667, Greenbelt, MD 20771, USA
[12] Christian-Albrechts-Universität zu Kiel, Institut für Theoretische Physik und Astrophysik, Leibnizstr. 15, 24098 Kiel, Germany
[13] Max-Planck Institut für Astronomie, Königstuhl 17, 69117 Heidelberg, Germany
[14] John Hopkins University, Dept. of Physics and Astronomy, 3701 San Martin drive, Baltimore, MD 21210, USA
[15] ESA Astrophysics & Fundamental Physics Missions Division, ESTEC/SRE-SA, Keplerlaan 1, 2201 AZ Noordwijk, The Netherlands
[16] INSA at ESAC, 28691 Villanueva de la Cañada, Madrid, Spain
[17] Onsala Space Observatory, Chalmers University of Technology, 439 92 Onsala, Sweden
[18] LESIA, Observatoire de Paris, 92195 Meudon Principal Cedex, France
[19] Department of Physics and Astrophysics, Open University, Walton Hall, Milton Keynes MK7 6AA, UK
[20] Rutherford Appleton Laboratory, Chilton OX11 0QX, UK

Received 8 February 2011 / Accepted 17 March 2011

ABSTRACT

Context. Dusty debris discs around main sequence stars are thought to be the result of continuous collisional grinding of planetesimals in the system. The majority of these systems are unresolved and analysis of the dust properties is limited by the lack of information regarding the dust location.

Aims. The *Herschel* DUNES key program is observing 133 nearby, Sun-like stars (<20 pc, FGK spectral type) in a volume limited survey to constrain the absolute incidence of cold dust around these stars by detection of far infrared excess emission at flux levels comparable to the Edgeworth-Kuiper belt (EKB).

Methods. We have observed the Sun-like star HD 207129 with *Herschel* PACS and SPIRE. In all three PACS bands we resolve a ring-like structure consistent with scattered light observations. Using α Boötis as a reference point spread function (PSF), we deconvolved the images, clearly resolving the inner gap in the disc at both 70 and 100 μm.

Results. We have resolved the dust-producing planetesimal belt of a debris disc at 100 μm for the first time. We measure the radial profile and fractional luminosity of the disc, and compare the values to those of discs around stars of similar age and/or spectral type, placing this disc in context of other resolved discs observed by *Herschel*/DUNES.

Key words. stars: individual: HD 207129 – circumstellar matter – infrared: stars

1. Introduction

Debris discs are composed of dust grains continuously produced by the collisional grinding of larger unseen planetesimals. This is inferred from the short lifetime of the dust grains compared to the age of the star (Backman & Paresce 1993) and suggest that the star around which they are observed has undergone a planetesimal formation process. In almost all cases, dust production is consistent with steady state attrition of the dust parent bodies (Löhne et al. 2008). The vast majority of debris discs are unresolved and we can only use modelling of the disc spectral energy distribution (SED) to determine the spatial location of the dust and the physical properties of the constituent dust grains. In the absence of independent information constraining

⋆ *Herschel* is an ESA space observatory with science instruments provided by European-led Principal Investigator consortia and with important participation from NASA.

⋆⋆ FNRS Postdoctoral Researcher.

the spatial location of the dust, which introduces degeneracies into the fitting of the dust grain properties, e.g. between grain size and radial location, a standard dust composition is assumed. In the few examples of resolved debris discs, structures that imply the presence of a planetary mass body to maintain and sculpt the disc are frequently observed, e.g. warps, asymmetries and blobs (Golimowski et al. 2006; Kalas et al. 2005; Sheret et al. 2004). Planets may also be responsible for the inner cavities seen in resolved discs and inferred from the SEDs of unresolved ones (Wyatt 2008). The resolved disc structure can therefore be used as an indirect probe for exoplanets around such stars in regions of orbital radius/planetary mass parameter space that are otherwise inaccessible to traditional search methods (e.g. radial velocity, transits) and remain a challenge to direct imaging techniques.

HD 207129 (HIP 107649) was identified as having a debris disc by *IRAS* (Walker & Wolstencroft 1988) and followed up by both *ISO* and *Spitzer* (Jourdain de Muizon et al. 1999; Trilling et al. 2008). Extended emission from the disc has been seen in both scattered light (*HST*) and in thermal infrared emission (*Spitzer* MIPS70, Krist et al. 2010). The disc excess was also detected at 160 μm by both Tanner et al. (2009) and Krist et al. (2010), though with very different values (155 mJy cf 250 mJy), illustrating the need for *Herschel* PACS observations to constrain the disc SED. Additionally, the system has been identified as a promising candidate for exoplanet searches, due to its proximity (16 pc), age (1–3 Gyr) and the presence of an inner gap in the disc (Jourdain de Muizon et al. 1999; Beichman et al. 2010).

In this paper we present *Herschel* (Pilbratt et al. 2010) PACS (Poglitsch et al. 2010) and SPIRE (Griffin et al. 2010) observations of HD 207129. The large aperture *Herschel* telescope provides arcsecond resolution allowing detailed imaging of the debris disc in this system. In addition, greater precision and denser coverage of the disc SED can be obtained. Altogether, this allows better constraints to be placed on the disc's SED and physical extent compared to previous observations, thereby allowing additional refinement of our models of this solar system analogue.

2. Observations and data reduction

HD 207129 was observed as part of the DUNES (DUst around NEarby Stars; Eiroa et al. 2010, Rodmann et al., in prep.) volume limited survey of nearby ($d < 20$ pc) Sun-like (FGK) stars. PACS scan map observations of the star were taken with both 70/160 and 100/160 channel combinations. Each scan map consisted of 10 legs of 3′ length, with a 4″ separation between legs, at the medium slew speed (20″ per second). The target was observed at two position angles (70 and 110°) in both wavelength combinations. SPIRE small map mode observations were also carried out on a separate observation day (OD) covering a region ~4′ around HD 207129 at the nominal slew speed (30″/s). Using five repetitions of the scan map observations reduced the expected noise level to close to that of the expected extragalactic contribution (7–9 mJy at 250–500 μm) and increased the coverage of the central region of the map allowing pixel sizes smaller than the standard values to be used in the image reconstruction process (i.e. image scales of 4″, 6″ and 8″ per pixel at 250, 350 and 500 μm, limited by the appearance of gaps in the image coverage near the centre of the map), which was useful for looking at extended structure in the source brightness profile. A summary of the observations is presented in Table 1.

Table 1. Summary of *Herschel* observations of HD 207129.

Instrument	Observation ID	OD	Wavelengths [μm]	Duration [s]
PACS	1342193163/64	322	70/160	276.0
PACS	1342193165/66	322	100/160	2250.0
SPIRE	1342209300	544	250/350/500	721.0

2.1. Herschel photometry

PACS data reduction was carried out in HIPE 4.2 (the latest available public release[1]), starting from the level 0 products using the standard reduction script. The separate scans at the two position angles of each channel pair were mosaiced to produce a final image at each wavelength. Image scales for the final mosaics were 1″ per pixel for the blue (70/100 μm) images and 2″ per pixel for the red (160 μm) image. A high-pass filter was used to remove large scale background emission from the images, with filter widths of 15 and 25″ in the blue and red channels, respectively. A central region of 30″ radius in the images was masked from the high pass filter process to prevent the removal of any faint extended structure near to the source. SPIRE data reduction was also carried out in HIPE 4.2, again starting from the level 0 data using the standard script and processing options. The SPIRE maps were created using the naive scan mapper alogrithm. The pixel scales for the SPIRE 250, 350 and 500 μm images from which photometry was taken were 6″, 10″ and 14″.

PACS fluxes were measured using aperture photometry carried out using the IDL APER routine. The aperture radius and sky annulus dimensions were 20″ and 30–40″, respectively. SPIRE fluxes were measured using an aperture of radius 30″ (due to the presence of several nearby sub-mm bright background objects), whilst the sky noise values were taken from Nguyen et al. (2010).

2.2. Stellar parameters

HD 207129 (HIP 107649) is a nearby ($d = 16 \pm 0.2$ pc, van Leeuwen 2007) star with a reported spectral type of G2V (from the *Hipparcos* catalogue, Perryman et al. 1997) or G0V (Gray et al. 2006). The bolometric luminosity has been estimated from the absolute magnitude and bolometric correction using measurements by Flower (1996). Our adopted values for the effective temperature, gravity and metallicity are derived from the mean of spectroscopic measurements from Santos et al. (2004), Valenti & Fischer (2005) and Sousa et al. (2008). Our own estimate of the rotational velocity, from high resolution spectra, is $\upsilon \sin i = 3.71 \pm 1.81$ km s^{-1} (Maldonado et al., in prep.), consistent with estimates of Groot et al. (1996) and Torres et al. (2006). Assuming the stellar inclination is that of the disc ($i = 60 \pm 5°$, see Sect. 3.2) and the stellar radius is 1.07 $R_{\odot}$ (estimated from the bolometric luminosity and effective temperature), the rotational period of the star is $P = 12.6$ days. The star is non-active, with measurements of the activity index, $\log R'_{\mathrm{HK}}$, of −4.8 Henry et al. (1996) and −5.02 Gray et al. (2006), and a *ROSAT* X-ray luminosity $\log L_{\mathrm{X}}/L_{\mathrm{bol}} = -5.63$.

The stellar mass estimated from the radius and gravity is 1.15 $M_{\odot}$. From Padova evolutionary tracks (Girardi et al. 2002), a mass of 1.0–1.1 $M_{\odot}$ and age of ~3.2 Gyr are obtained. This age is consistent with the activity index of Henry et al. (1996), using the calibration from Mamajek & Hillenbrand (2008).

[1] see: http://herschel.esac.esa.int/HIPE_download.shtml

Conversely, the age derived from the rotational period using the same calibration is ∼1.6 Gyr, which is consistent with the X-ray luminosity age of 1.8 Gyr using the relationship of Garcés et al. (2010), or the results of Giardino et al. (2008) (their Fig. 8). Other age estimates range from 0.6 (Song et al. 2003) to 6.0 Gyr (Lachaume et al. 1999; Valenti & Fischer 2005; Holmberg et al. 2009). We measure a LiI 6708 Å equivalent width of 35.5 ± 3.3 mÅ (Maldonado et al., in prep.); this value, in conjunction with the estimate derived from the rotation period, points to an age greater than 600 Myr, implying the stellar age lies between these extremes. We therefore adopt an age in the range 1.5–3.2 Gyr as appropriate for HD 207129 (see Figs. 6 and 9, Maldonado et al. 2010). The stellar parameters and observational properties are summarised in Table 3.

The stellar photosphere contribution to the total flux was computed, using the stellar parameters, from a synthetic stellar atmosphere model interpolated from the PHOENIX/GAIA grid (Brott & Hauschildt 2005). Optical and near infrared photometry including Stromgren *uvby*, Tycho-2 *BV* and *JHK* from Aumann & Probst (1991) constrain the stellar component of the SED, which has been scaled to the *Spitzer* IRS spectrum following the method of Bertone et al. (2004).

3. Results

3.1. Disc spectral energy distribution

For the purposes of disc SED modelling, the PACS photometry was supplemented by a broad range of infrared and sub-millimetre observations including *AKARI* IRC all-sky survey 9/18 μm (Ishihara et al. 2010), *Spitzer* IRS spectrum and MIPS 24 and 70 μm photometry (Trilling et al. 2008), *Spitzer* 160 μm (Krist et al. 2010), APEX/LABOCA 870 μm (Nilsson et al. 2010) fluxes and upper limits from 450/850 μm JCMT/SCUBA (Sheret et al. 2004) and 1.2 mm SEST (Schütz et al. 2005) observations. The *Herschel* photometry and all complementary data are summarised in Table 2 (the upper limits are not quoted in the table because they were not used in the SED fitting process).

The disc SED, with the *Herschel* fluxes and ancillary photometry can be seen in Fig 1. We have fitted the excess emission from HD 207129 with a standard black body model, modified beyond 210 μm by a factor of $\beta = 1$ (see Eq. (6), Wyatt 2008), from which estimates of the disc fractional luminosity and disc orbital radius were derived. The model was fitted to the infrared (both *Herschel* and ancillary) photometry through least squares minimisation weighted by the observational uncertainties. The best fit temperature $T_{\rm disc}$ = 50 K and fractional luminosity $L_{\rm IR}/L_{\rm Bol} = 8.3 \times 10^{-5}$ were obtained with a reduced χ^2 of 1.34. Using the derived stellar parameters and the typical disc temperature, we calculate a dust orbital radius of 34 AU for black body emission, clearly much smaller than the resolved disc which would imply that a disc orbital radius larger than that derived from the black body modelling is required.

3.2. Disc images

The disc of HD 207129 is clearly resolved in the PACS mosaics at all three wavelengths and is extended in the two shorter SPIRE wavelength maps. The optical position of HD 207129 is (in the epoch of the *Herschel* images) $21^{\rm h}48^{\rm m}16.05^{\rm s}$ $-47°18'14.47''$ (using proper motions from the re-reduction of *Hipparcos*, van Leeuwen 2007). In the PACS 70 μm image there is a peak in the disc brightness ∼2″ NE from this position, consistent with the optical position within the *Herschel* pointing uncertainty, with a flux value consistent with the predicted stellar photosphere contribution. If this peak were the star, that would imply that the disc was asymmetric. In the deconvolution presented here, we have assumed that the star is at the centre of the disc, consistent with the symmetric scattered light disc observed in the *HST* results (Krist et al. 2010), and that the peak observed in the 70 μm image is a dust blob.

The disc size and position angle were measured by fitting a rotated ellipse to the source brightness profile contour of 3 times the sky noise value in the PACS images, whilst the disc inclination is measured from the ratio of the semi-minor to semi-major axes. A summary of these properties is in Table 4. The disc extent is the same in both the 70 and 100 μm images, though we would naively expect that the apparent disc size would increase due to the larger beam size and greater contribution from colder dust emission. We attribute the similar disc sizes to a

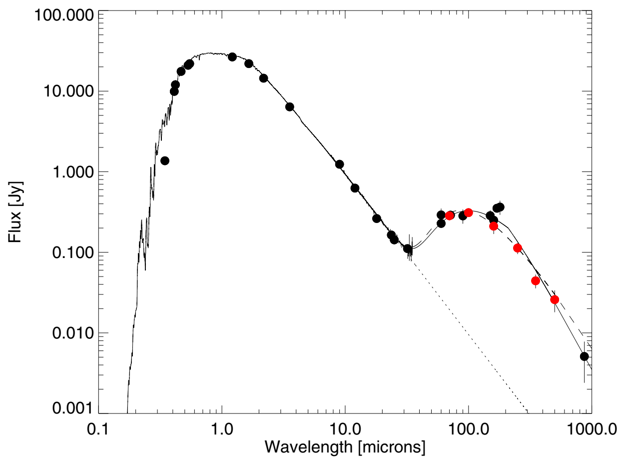

Fig. 1. HD 207129 spectral energy distribution. Red data points are the PACS and SPIRE photometry, black data points are the ancillary data, including the *Spitzer* IRS spectrum. Error bars are 1 σ and include both calibration uncertainty (10% for 70/100 μm, 20% for 160 μm) and sky noise. Some error bars are smaller than the data point symbol. For wavelengths longer than ∼30 μm the solid line represents a disc model with a λ_0 = 210 μm and β = 1, the dashed line represents a disc model with a λ_0 = 63 μm and β = 2.7 and the dotted line represent the stellar photosphere.

Table 2. Summary of *Herschel* and ancillary infrared/sub-mm photometry used in disc SED fitting.

Wavelength [μm]	$F_{\rm obs}$ [mJy]	Instrument
9	1237 ± 17	*AKARI*/IRC PSC, Ishihara et al. (2010)
18	263 ± 31	*AKARI*/IRC PSC, Ishihara et al. (2010)
24	155 ± 5.3	*Spitzer*/MIPS, Trilling et al. (2008).
32	111 ± 5.1	*Spitzer*/IRS
70	278 ± 11	*Spitzer*/MIPS, Trilling et al. (2008)
160	250 ± 40	*Spitzer*/MIPS, Krist et al. (2010)
160	158 ± 20	*Spitzer*/MIPS, Tanner et al. (2009)
70	284 ± 1.5	*Herschel*/PACS
100	311 ± 1.1	*Herschel*/PACS
160	211 ± 1.5	*Herschel*/PACS
250	113 ± 18	*Herschel*/SPIRE
350	44.3 ± 9	*Herschel*/SPIRE
500	25.9 ± 8	*Herschel*/SPIRE
870	5 ± 3	APEX/LABOCA, Nilsson et al. (2010)

Notes. Uncertainties 1-σ and driven by the sky noise. *Herschel* calibration uncertainties are 10% for PACS and 15% for SPIRE.

Table 3. Physical properties of HD 207129.

Parameter	Value
Distance	16 ± 0.2 pc
Spectral type and luminosity class	G2V, G0V
V, $B-V$	5.57, 0.60 mag
Absolute magnitude M_V, bolometric correction	4.55, –0.06
Bolometric luminosity, L_*	1.258 $L_\odot$
Effective temperature	5912 K
Surface gravity, $\log g$	4.44
Radius, R_*	1.07 $R_\odot$
Metallicity, [Fe/H]	–0.01
Rotational velocity, $\upsilon \sin i$	3.71 km s^{-1}
Rotation period, P	~12.6 days
Activity, $\log R'_{\rm HK}$	–4.80, –5.02
X-Ray luminosity, $\log\ L_{\rm X}/L_*$	–5.63
Mass, M_*	1.0–1.15 $M_\odot$
Age	1.5–3.2 Gyr

Table 4. Measurement of the disc extent before (left – the HWHM of a Gaussian fitted to the source brightness profile) and after (right – the radial extent of annulus peak brightness) deconvolution, and the inclination and position angle of the disc at all three wavelengths.

	Wavelength					
	70 μm		100 μm		160 μm	
Semi-major axis [″]	14.5	9.0	14.0	9.0	17.0	8.5
Semi-major axis [AU]	232	144	224	144	272	136
Semi-minor axis [″]	8.5	4.0	8.5	4.5	12.0	4.0
Semi-minor axis [AU]	136	64	136	72	192.0	64
Position angle[a] [°]	120		122		120	
Inclination[b] [°]	54	64	53	60	45	62

Notes. [(a)] The disc position angles are the same in both original and deconvolved images. [(b)] The disc minor axis is not resolved at 160 μm in the original images.

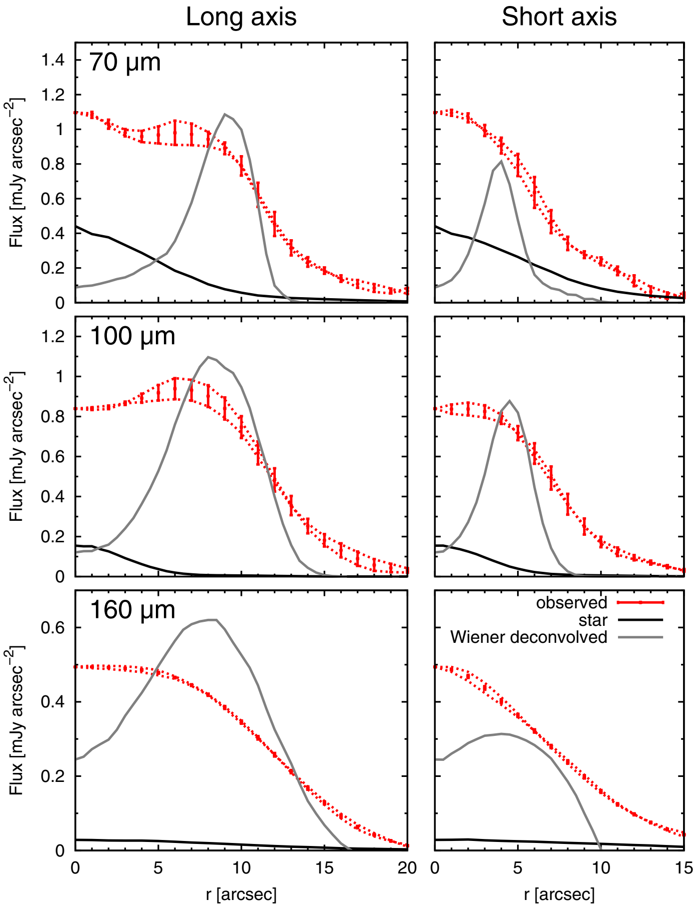

Fig. 2. Radial profiles of HD 207129 along the semi-major (*left*) and semi-minor (*right*) axes of the disc. The red dotted lines are the measured profile either side of the disc centre along each axis; the solid red error bars mark the mean position at each point and the associated uncertainty. The grey line is the deconvolved disc profile and the black line is the subtracted stellar profile.

combination of the similar beam sizes at the two wavelengths (5.7″ and 6.7″ *FWHM* at 70 and 100 μm, respectively) which are both small compared to the extent of the disc. In both the 70 μm and 100 μm image, there are two peaks in the source brightness profile, with the NW peak ~10% brighter than the SE one (at 100 μm). This structure is consistent with the underlying disc being a symmetric ring-like structure. Additionally at 70 μm, there is a third peak close to the centre of the disc, which is NE (~2″) of the disc centre and stellar position, which may be the result of inhomogenities in the disc structure. The disc source brightness profile at 160 μm (and in the SPIRE images) is smooth, showing no internal structure.

In order to measure the true extent of the disc, the images were deconvolved from the instrument PSF, a technique which has previously proved successful (Liseau et al. 2010). An observation of α Boötis was used as the PSF model for the deconvolution, rotated to match the roll angle of the telescope at the time of observing HD 207129.

Deconvolution was a two step process; the stellar photosphere contribution was removed from each image by subtraction of a PSF with a peak scaled to the predicted photospheric flux level in that image and centred on the stellar position determined from measurement of the 70 μm isophotes. The optical and isophote derived positions are in good agreement and the small offset between them does not impact upon the findings of this analysis.

After star subtraction, the image was deconvolved using three separate methods (modified Wiener, Richardson-Lucy and van Cittert) to check the suitability of the individual methods and the repeatability of any structure observed in the deconvolved images. It was found that all three methods clearly produced a ring structure in the deconvolved 70 and 100 μm images, though with varying noise patterns. Deconvolution of the 160 μm image via modified Wiener and van Cittert methods resulted in images with the disc structure as a pair of blobs either side of the stellar position. Using the Richardson-Lucy method the disc structure at 160 μm was recovered as a broken ring surrounding the stellar position with a clear central gap. We do not interpret the clumpy blobs in the deconvolved disc images as representing real structure in the debris disc. The result of the image deconvolution using the modified Wiener method can be seen in Fig. 3.

The deconvolved radial extent of the disc was measured from the position of the peak brightness of the observed disc annulus along its major and minor axes. In the deconvolved 100 μm image, the measured radial extent was 9″ ± 2″ (144 ± 32 AU, see Fig. 2), with similar values from the 70 and 160 μm images. We measure the position angle of the disc to be 120 ± 5° through fitting via a least squares minimisation algorithm. From the ratio of the semi-major and semi-minor axes, the inclination to be 54 ± 5° (60 ± 5° in the deconvolved images). These results are consistent with previous *HST* measurements (Krist et al. 2010). We see no shift in the positional angle of the disc toward longer wavelengths.

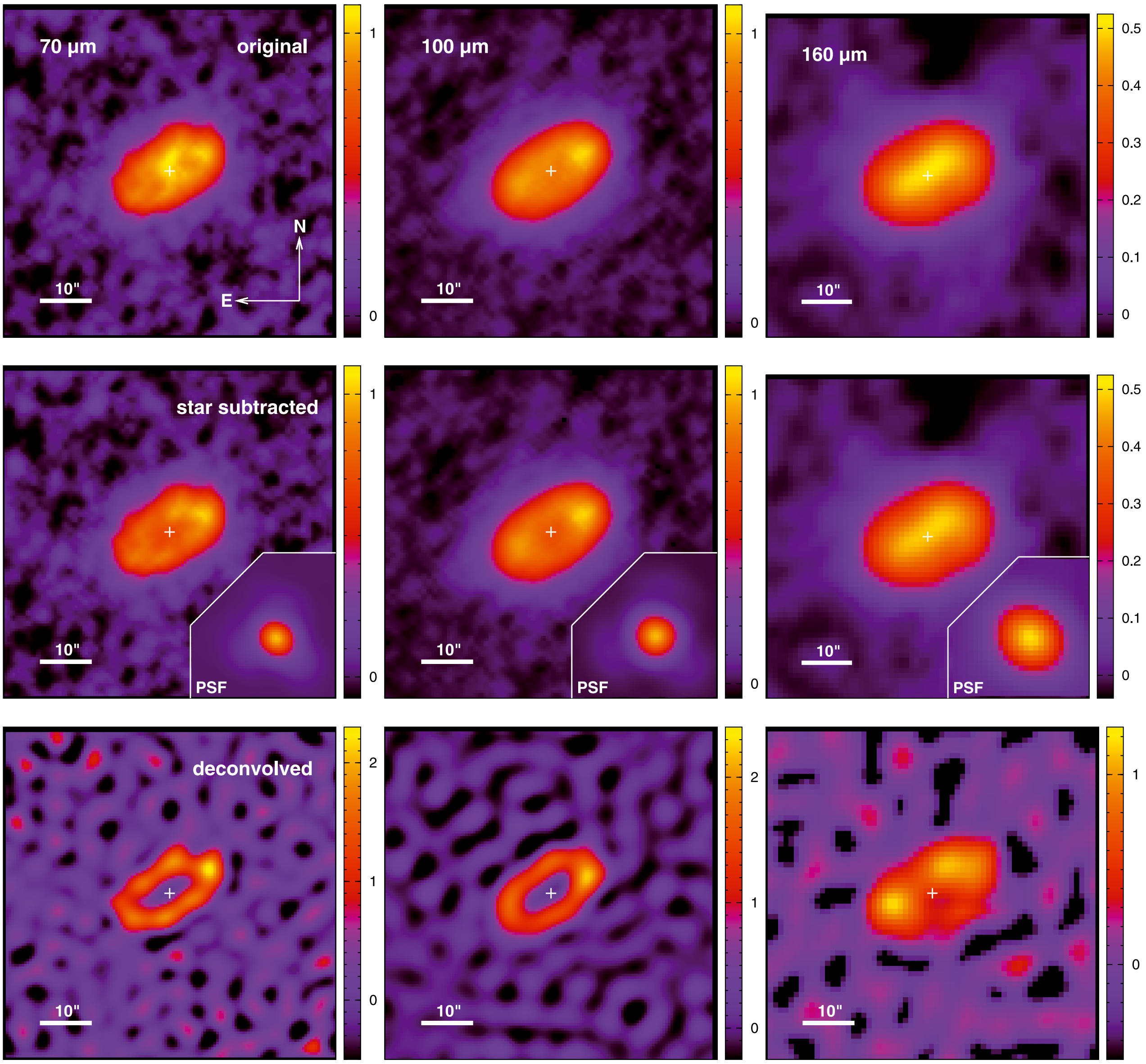

Fig. 3. Original image (*top*), post stellar subtraction (*middle*) and Wiener deconvolved image (*bottom*) in the three PACS wavelengths. The ring structure is clearly visible in both the 70 and 100 μm images. Image orientation is North up, East left. A distance scale bar has been provided, 10″ is equivalent to 160 AU. The colour scale bar is in units of mJy/arcsec^2. The stellar position, derived from isophotes in the 70 and 100 μm observations, is marked as a white cross in each image.

3.3. Discussion

We have directly resolved the structure of a ring-like debris disc for the first time in the far infrared. The disc radial extent of ~140 AU is comparable to that of Fomalhaut (Kalas et al. 2005) or HD 107146 (Ardila et al. 2004).

The disc radius derived from the standard black body model, modified beyond 210 μm by a factor of $\beta = 1$, was 34 AU. This is a large underestimate of the true extent, in direct conflict with the resolved images. It serves to illustrate the dangers of modelling debris discs using only the SED and/or black body thermal emission models, which neither assume, nor tell you anything about, the dust grain optical properties (Wyatt 2008). Using a disc of dust grains that emit as modified black bodies and 10 μm dust grains, with a break shortward of the SED peak, the disc radius derived from the SED matches the observed images but fails to reproduce the sub-millimetre slope. The observed dust optical and thermal emission properties cannot be reconciled via Mie theory, either. A disc composed of small (<1 μm) dust grains would, according to Mie theory, reproduce the symmetric scattered light image, though the dust would then be too warm to reproduce the SED (Krist et al. 2010).

We measure a dust fractional luminosity of 8.3×10^{-5}, around six times greater than Vega (1.5×10^{-5}, Habing et al. 2001) and half that of q^1 Eri (1.5×10^{-4}, Liseau et al. 2008). The value we measure is consistent with the fractional luminosity/age relation from Decin et al. (2003). The disc extent, ~140 AU, is larger than other DUNES resolved discs, e.g. q^1 Eri (85 AU, Liseau et al. 2010) or ζ^2 Ret (70–120 AU, Eiroa et al. 2010), but the derived black body temperature is also large, ~50 K, cf 60 K for the q^1 Eri disc which is around an F star and 30–40 K for the ζ^2 Ret disc which has a smaller extent around a star of similar spectral type.

A complete analysis of the disc SED and physical structure, in which both classical power-law particle size distribution models and a self-consistent collisional model are fitted to the available photometric and imaging data will be presented by Löhne et al. (in prep.).

4. Conclusions

We have presented *Herschel* PACS and SPIRE observations of HD 207129, the first to directly resolve the ring-like structure of a debris disc in both major and minor axes at far infrared wavelengths. The disc extent (140 ± 32 AU), inclination ($51 \pm 5°$) and typical (black body) temperature (~50 K), derived purely from the observations assuming no particular grain model, are similar to previous measurements. Compared to other discs around stars of similar spectral type and age, the disc of HD 207129 is both larger and warmer (for the observed size), though it is not completely atypical in either respect, but situated at the margins of the known range of disc morphologies. A simple analysis based on a black body model has been proved unrealistic. A more detailed self-consistent study is left for future work (Löhne et al., in prep.).

Acknowledgements. We would like to thank the staff at the Herschel Science Centre, discussions with whom added immeasurably to the quality of the data reduction. C. Eiroa, J. Maldonado, J.P. Marshall, and B. Montesinos are partly supported by Spanish grant AYA 2008/01727. T. Löhne, S. Müller and A. Krivov acknowledge support by the DFG, projects Lo 1715/1-1 and Kr 2164/9-1. J.-Ch. Augereau, J. Lebreton and P. Thébault are supported by a CNES-PNP grant.

References

Ardila, D. R., Golimowski, D. A., Krist, J. E., et al. 2004, ApJ, 617, L147
Aumann, H. H., & Probst, R. G. 1991, ApJ, 368, 264
Backman, D. E., & Paresce, F. 1993, in Protostars and Planets III, ed. E. H. Levy, & J. I. Lunine, 1253
Beichman, C. A., Krist, J., Trauger, J. T., et al. 2010, PASP, 122, 162
Bertone, E., Buzzoni, A., Chávez, M., & Rodríguez-Merino, L. H. 2004, AJ, 128, 829
Brott, I., & Hauschildt, P. H. 2005, in The Three-Dimensional Universe with Gaia, ed. C. Turon, K. S. O'Flaherty, & M. A. C. Perryman, ESA SP-576, 565
Decin, G., Dominik, C., Waters, L. B. F. M., & Waelkens, C. 2003, ApJ, 598, 636
Eiroa, C., Fedele, D., Maldonado, J., et al. 2010, A&A, 518, L131
Flower, P. J. 1996, ApJ, 469, 355
Garcés, A., Ribas, I., & Catalán, S. 2010, in ASP Conf. Ser., 430, ed. V. Coudé Du Foresto, D. M. Gelino, & I. Ribas, 437
Giardino, G., Pillitteri, I., Favata, F., & Micela, G. 2008, A&A, 490, 113
Girardi, L., Bertelli, G., Bressan, A., et al. 2002, A&A, 391, 195
Golimowski, D. A., Ardila, D. R., Krist, J. E., et al. 2006, AJ, 131, 3109
Gray, R. O., Corbally, C. J., Garrison, R. F., et al. 2006, AJ, 132, 161
Griffin, M. J., Abergel, A., Abreu, A., et al. 2010, A&A, 518, L3
Groot, P. J., Piters, A. J. M., & van Paradijs, J. 1996, A&AS, 118, 545
Habing, H. J., Dominik, C., Jourdain de Muizon, M., et al. 2001, A&A, 365, 545
Henry, T. J., Soderblom, D. R., Donahue, R. A., & Baliunas, S. L. 1996, AJ, 111, 439
Holmberg, J., Nordström, B., & Andersen, J. 2009, A&A, 501, 941
Ishihara, D., Onaka, T., Kataza, H., et al. 2010, A&A, 514, A1
Jourdain de Muizon, M., Laureijs, R. J., Dominik, C., et al. 1999, A&A, 350, 875
Kalas, P., Graham, J. R., & Clampin, M. 2005, Nature, 435, 1067
Krist, J. E., Stapelfeldt, K. R., Bryden, G., et al. 2010, AJ, 140, 1051
Lachaume, R., Dominik, C., Lanz, T., & Habing, H. J. 1999, A&A, 348, 897
Liseau, R., Risacher, C., Brandeker, A., et al. 2008, A&A, 480, L47
Liseau, R., Eiroa, C., Fedele, D., et al. 2010, A&A, 518, L132
Löhne, T., Krivov, A. V., & Rodmann, J. 2008, ApJ, 673, 1123
Maldonado, J., Martínez-Arnáiz, R. M., Eiroa, C., Montes, D., & Montesinos, B. 2010, A&A, 521, A12
Mamajek, E. E., & Hillenbrand, L. A. 2008, ApJ, 687, 1264
Nguyen, H. T., Schulz, B., Levenson, L., et al. 2010, A&A, 518, L5
Nilsson, R., Liseau, R., Brandeker, A., et al. 2010, A&A, 518, A40
Perryman, M. A. C., Lindegren, L., Kovalevsky, J., et al. 1997, A&A, 323, L49
Pilbratt, G. L., Riedinger, J. R., Passvogel, T., et al. 2010, A&A, 518, L1
Poglitsch, A., Waelkens, C., Geis, N., et al. 2010, A&A, 518, L2
Santos, N. C., Israelian, G., & Mayor, M. 2004, A&A, 415, 1153
Schütz, O., Meeus, G., & Sterzik, M. F. 2005, A&A, 431, 175
Sheret, I., Dent, W. R. F., & Wyatt, M. C. 2004, MNRAS, 348, 1282
Song, I., Zuckerman, B., & Bessell, M. S. 2003, ApJ, 599, 342
Sousa, S. G., Santos, N. C., Mayor, M., et al. 2008, A&A, 487, 373
Tanner, A., Beichman, C., Bryden, G., Lisse, C., & Lawler, S. 2009, ApJ, 704, 109
Torres, C. A. O., Quast, G. R., da Silva, L., et al. 2006, A&A, 460, 695
Trilling, D. E., Bryden, G., Beichman, C. A., et al. 2008, ApJ, 674, 1086
Valenti, J. A., & Fischer, D. A. 2005, ApJS, 159, 141
van Leeuwen, F. 2007, A&A, 474, 653
Walker, H. J., & Wolstencroft, R. D. 1988, PASP, 100, 1509
Wyatt, M. C. 2008, ARA&A, 46, 339